Bulgarian Chemical Communications, Volume 49 Special Issue C (pp. 119– 127) 2017

Application of Stoynov's 4-D analysis for nonstationary impedance spectra corrections of thin poly(*o*-ethoxyaniline) modified Pt electrode

V. Horvat-Radošević*, K. Kvastek, K. Magdić Košiček

Division for Marine and Environmental Research, Rudjer Bošković Institute, Bijenička c. 54, 10000 Zagreb, Croatia

Received November 18, 2016 Revised January 02, 2017

Stoynov's 4-D analysis has been applied for corrections of nonstationary impedance spectra of poly(o-ethoxyaniline) POEA modified Pt electrode measured using conventional EIS technique at the potential of conducting to insulating conversion of polymer. The series of nine sequentially measured impedance spectra of Pt/POEA electrode showed significant increase with operating time of experiment, implying not only time-varying system but also nonstationarity, *i.e*. time changes within time interval of the single impedance spectrum measurement. Correction procedure for nonstationarity, comprising three mathematical steps, was applied to each of sequentially measured impedance spectrum. In the first step of the procedure, central times of data acquistion at each frequency point were determined, referred to the operating time of experiment and as the fourth variable included into impedance data sets of all experimentally measured IS. In the second step of the procedure, the operating time function of measured real and imaginary impedance parts at iso-frequency points was built up and "frozen" at starting times of each impedance spectrum measurement. In the last step of the procedure, nine instantaneous impedance spectra were calculated using extrapolation/interpolation method. Comparison between measured and instantaneous impedance spectra showed differences that indicate overestimation of all charge transfer and charge transport resistances and underestimation of charge pseudocapacitance values for not corrected *vs*. corrected IS of Pt/POEA electrode. .

Key words: electrochemical impedance spectroscopy, Stoynov's 4-D analysis, nonstationarity, poly(*o*-ethoxyaniline) modified electrode.

INTRODUCTION

Electrochemical impedance spectroscopy (EIS) is a frequency domain technique based on the transfer function concept defining the input-output relation for a linear, time invariant, casual and stable system [1–6]. For a small signal sinusoidal current fluctuation $i(t)$ as the system input and the resulting small signal sinusoidal voltage fluctuation $v(t)$ as the output, the impedance Z is defined in the complex frequency, iμ domain as the system transfer function relating Fourier-transformed F forms of $i(t)$ and $v(t)$:

$$Z(\mathrm{i}\mu)=F[v(t)]/F[i(t)=V(\mathrm{i}\mu)/I(\mathrm{i}\mu)=|Z|exp^{i\varphi}=Z'+\mathrm{i}Z'' \quad (1)$$

Impedance spectra of electrochemical systems in steady-state have conventionally been measured by the frequency response analysis (FRA) technique, carried out frequency by frequency at n points, covering wide range of time (10^{-5} – 10^{3} s). At each frequency μ, vector properties of impedance have been defined according to eq. (1) by impedance modulus $|Z|$ and phase angle ¨, or real Z' and imaginary Z" impedance components, respectively. The collected three-dimensional (3-D) measured data set ($Z'_{(n)}$, $Z''_{(n)}$, $\mu_{(n)}$) contains all the informaton of the system properties, which in the form of impedance parameter values might be extracted by impedance modeling procedure [1–6]. In practice, however, measured electrochemical systems are usually nonlinear, noisy and nonstationary, what prevents proper evaluation of impedance values and thus properties of the measured system. There have been several procedures already proposed for avoiding these problems, including application of selected input signal amplitude, measurements and analysis of non-linear and higher order voltage harmonics, pulse, multisinusoidal or pseudo-white noise excitations, etc. [7–11].

The present paper is focused to the problem of nonstationarity that is common for many electrochemical systems in either two-electrode or three-electrode configurations [8,10,12–17]. In conventional, FRA measured impedance spectra, nonstationarity is usually manifested as drifts of experimental impedance spectra measured sequentially. Drifts can be found on different time scales, most usually at low frequencies, altering thus effective characteristics of the system between two subsequent experiments. Reasons for drifts are different, ranging from departure from the causality condition to time changes inherent to a system

To whom all correspondence should be sent:
E-mail: vhorvat@irb.hr

under investigation. Time changes of a system are usually generated by changes of electrode surfaces caused by different phenomena such as erosion-corrosion, various structural relaxations or load changes as in batteries and fuel cells during operation [18–21]. Several numerical procedures for correction of conventionally measured EIS data upon nonstationary conditions and elimination of drifts have already been proposed, resulting in highly relevant impedance data for system characterization [20,21]. Almost all these procedures are actually based on the simple and powerful method developed by Stoynov [12–14] and known as the four-dimensional, 4-D impedance analysis. According to Stoynov's 4-D impedance analysis, duration of measurement, including time of data acquisition at every μ point, generates additional variable which makes the measured data set for a time evolving system determined by four variables. Thus, the standard 3-D data set ($Z'_{(n)}$, $Z''_{(n)}$, $\mu_{(n)}$) is enhanced to 4-D by the fourth variable $t_{(n)}$, defined as central time of measurement at each $\mu_{(n)}$. By realizing a series of impedance measurements at distinct time intervals giving 4-D experimental data sets ($Z'_{(n)}$, $Z''_{(n)}$, $\mu_{(n)}$, $t_{(n)}$), impedance spectra can be numerically reconstructed for some strictly defined moment of time, than turned back to standard 3-D data sets and parametrized by standard procedures. In combination with differential impedance analysis, DIA [22], 4-D impedance analysis defined a new technique, known as nonstationary differential impedance spectroscopy NODIS [23]. 4-D analysis and/or NODIS have already been applied to impedance analyses of hydrogen underpotential deposition and battery cycling [23,24].

In the present study, Stoynov's 4-D analysis will be applied for correction of time evolved impedance spectra of poly-*o*-ethoxyaniline (POEA) film modified Pt electrode, measured at the potential of polymer redox transition. POEA is the ring-substituted polyaniline (PANI) derivative with $-OC_2H_5$ groups [25] that together with PANI belongs to the class of intrinsic conducting organic polymers (ICPs) [26]. ICPs are materials of high potential and actual applications, mostly due to ability of fast switching from insulating to conducting state and *vice versa*. Electrochemical switching of ICPs, including PANI and its derivatives, is basically electrochemical oxidation/ reduction coupled by ionic (proton or counterion) egress/ingress. Switching reaction involves a number of underlying processes which were found to be different in time scale and dependent on the switching direction [27–29]. This, together with the irreversible degradation of PANI found prominent at some circumstances [30,31], have implied that for PANI based electrodes time invariant impedance spectra can hardly be assured. Although some adapted EIS techniques giving instantaneous impedance spectra have already been applied to PANI electrodes [32,33], the conventional EIS has been used for a long time [34–42] and still proposed [43,44] for assessment of charge storage and charge transfer/transport processes in PANI based polymer films. Conventional EIS, however, has primarily been explored for characterization of PANI and its derivatives in their conducting state [34–39] where all relaxations are generally fast, diminishing thus a probability for nonstationarity. Even for the conducting state of PANI in some conditions [40,41] and particularly at potentials of conductor to insulator or inverse conversions [42], nonstationary impedance spectra have actually been measured, needing necessary corrections for obtaining real impedance parameter values. In this work, corrections of nonstationary impedance spectra measured for the POEA modified Pt electrode at the specific potential of conducting to insulating conversion in the sulphuric acid solution will be performed using the mathematical treatment of Stoynov's 4-D analysis [12–14,24]. It must be stressed here, that such a type of correction has not been performed to impedance spectra of PANI based electrodes heretofore.

EXPERIMENTAL

Electrochemical cell and solutions

In the present measurements, three-electrode cell filled with 0.5 mol dm^{-3} H_2SO_4 (Kemika, 96%) electrolyte solution (pH = 0.5) was explored. Pt wire of 0.09 cm^2 geometric area served as the working electrode. High surface Pt-spiral in the separate compartment and Luggin capillary ended saturated calomel electrode (SCE) were used as the counter and reference electrodes, respectively. The pseudo-reference electrode in the form of Pt-probe put across Luggin capillary served for diminishing contributions of experimental artefacts to high frequency parts of impedance spectra [45]. All here mentioned potentials *E* are referred to the SCE. Electrochemical measurements were performed at room temperature with solution being deoxygenated by purging high purity N_2 for at least 15 minutes before the start of every experiment.

Preparation of Pt/POEA electrode

Pt/POEA electrode was prepared by potentiodynamic growth of POEA at the Pt wire

substrate from the monomer solution containing 0.5 mol dm^{-3} o-ethoxyaniline (Aldrich, p.a.) (previously distilled under reduced pressure) and 0.5 mol dm^{-3} H_2SO_4 [38,46]. Potential was cycled continuously at the scan rate of 50 mV s^{-1} between –0.20 and 1.00 V using Solartron 1287 Electrochemical Interface (ECI) under CorrWare (Scribner Assoc.) software control. After passing of three potential cycles, the synthesis procedure was stopped at –0.20 V, Pt/POEA electrode was extracted from the cell, rinsed in 0.5 mol dm^{-3} H_2SO_4 and transferred to newly prepared deareated and o-ethoxyaniline free 0.5 mol dm^{-3} H_2SO_4. The electrode was then submitted to four cyclic voltammetry scans between –0.15 and 0.40 V at scan rate of 50 mV s^{-1}, where the polymer was switched from insulating leucoemeraldine (LE) to conducting emeraldine (EM) form and vice versa [38,46]. Charge density, q_a = 30 mC cm^{-2} necessary for switching LE to EM was calculated by integrating the area under anodic current peak [38,46,47] indicating formation of thin polymer film (q_a <150 mC cm^{-2}) [47]. CV scanning was finished at –0.15 V and Pt/POEA electrode was held at this potential overnight prior to its transformation to EM state performed by the potential step oxidation at 0.30 V.

Impedance spectra measurements

Impedance spectra (IS) measurements were carried out using the Solartron equipment with 1287 ECI and 1255B FRA under Z_{plot} (Scribner Assoc.) software control. At selected voltage, a sine wave ac signal of 10 mV amplitude was imposed between 10^5 Hz and 0.01 Hz and 10 impedance points were measured per decade, resulting in 71 frequency points $f_{(1\text{-}71)} = \omega_{(1\text{-}71)}/2\pi$. Integration time t_{in} = 10 s at each frequency point and time delay t_d = 1 s before start of every consequtive frequency measurement were pre-selected.

Fig. 1 displays the duration t_m of data acquisition for each of the 71 frequency points of a single IS measured in the above given conditions.

As can be seen in the inset of Fig. 1 where t_m of the first three frequency points are enlarged, the measurement at each frequency point has its beginning (t_s), central (t_c) and ending (t_e) time, all referred to the starting time of the corresponding IS measurement at $f_{(1)} = 10^5$ Hz. Although t_m is generally defined as the sum of pre-selected t_{in} and t_d, Fig. 1 shows that at f < 0.1 Hz, t_m becomes longer than 11 s. The measurement time of one IS (T_m) took 1182 s (19.7 min) to complete, with about half of T_m spent for measurements at f < 0.1 Hz.

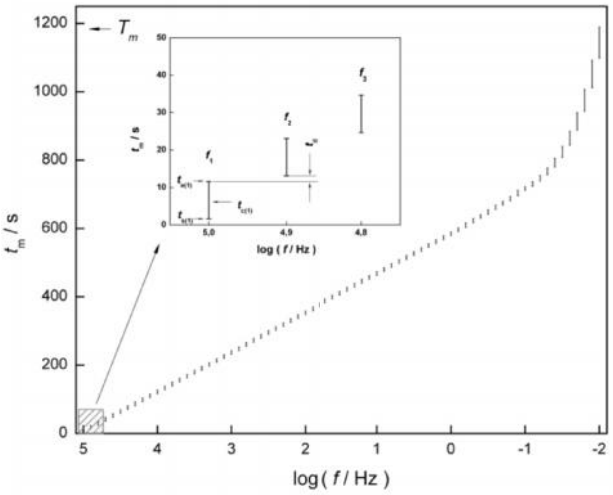

Fig. 1. Duration of the single frequency measurement time t_m under the given conditions of IS measurements at each of the 71 frequency points explored.

In the present experiment, IS of the Pt/POEA electrodes were measured as the series of 9 sequential measurements after the potential was stepped in the negative direction from 0.30 V (EM state) to 0.05 V (EM→LE conversion state). Principle time program of sequential IS measurements is presented in Fig. 2.

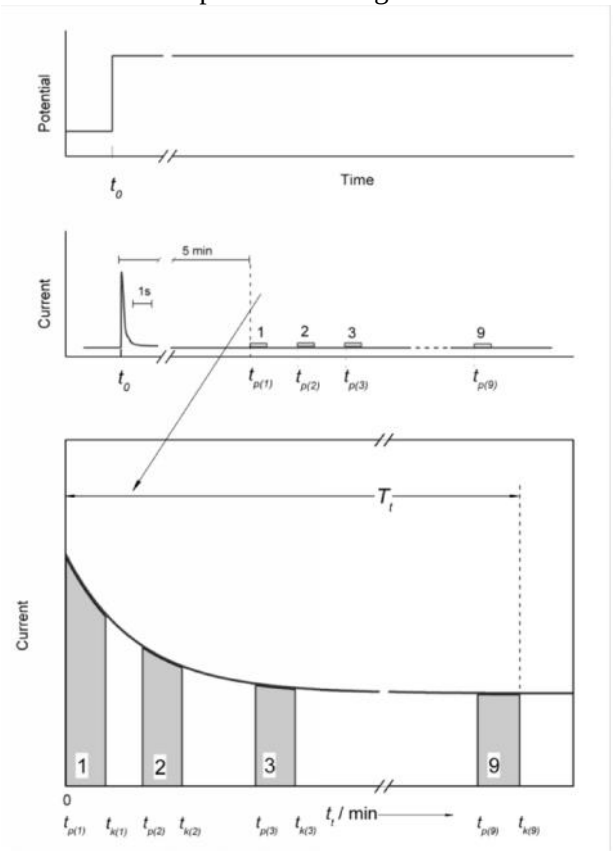

Fig. 2. Principle time program of 9 sequential IS measurements in the performed experiment.

As designated by small rectangles in the medium part of Fig. 2, the series of 9 sequential IS measurements commenced after the impose of potential step (upper part of Fig. 2), defining t_o as the moment when measurement of current transient has started. The first IS measurement started 5 min later (when current transient fully vanished) at time $t_{p(1)}$, while subsequent IS measurements started at $t_{p(2)}$ to $t_{p(9)}$ with some time left between them. By referring operative time of the impedance experiment t_t to $t_{p(1)}$ =0, the undermost part of Fig. 2 is obtained. Here, the starting t_p and ending t_k time of IS measurements are denoted and T_m of each IS is shadowed. At the end of the full experiment after total operating time T_t = 540 min, 9 impedance spectra were totally obtained, each composed from 71 4-D data sets (Z_m'$_{(1-71)}$, Z_m"$_{(1-71)}$, $\mu_{(1-71)}$, $t_{e(1-71)}$). According to Fig. 1 and Table 1 that summarizes definitions and abbreviations of all time symbols used here, $t_{e(1-71)}$ denotes ending time of measurement at each one of the 71 frequency points. Since t_e at each frequency is referred to the start of the corresponding IS measurement ($t_{p(1)}$ to $t_{p(9)}$), the values of t_e are equal for each of the sequentially measured IS.

Table 1. Time definitions and abbreviations.

t_0	Starting time of current transient measurement after potential step
	SINGLE IS
$t_{s(1-71)}$	Starting time of data acquisition at each frequency point (1–71)
$t_{e(1-71)}$	Ending time of data acquisition at each frequency point (1–71)
$t_{c(1-71)}$	Central time of data acquisition at each frequency point (1–71)
t_{in}	Integration time of data acquisition at each frequency point (1–71)
t_d	Time delay before start of data acquisition at consecutive frequency point
t_m	Time of data acquisition at each frequency point
T_m	Time of data acquisition at all frequency points of single IS spectra
	SERIES OF SEQUENTIAL IS
$t_{p(1-9)}$	Starting time of each IS measurement
$t_{k(1-9)}$	Ending time of each IS measurement
t_t	Operating time of the experiment referred to $t_{p(1)}$=0
T_t	Total operating time of the experiment
t^*	„Frozen" time (at $t_{p(1-9)}$ =0)

Calculations and fittings

All calculations related to the non-linear (NNL) data fittings of the built-in function for time dependence of impedance (ExpAssoc), determination of corresponding parameters and subsequent extrapolation/interpolations were made by the Origin (Origin Lab. Incorp.) software. Statistical criteria for reasonable fits were set as acceptable chi-square ¡^{2} test for goodness of the overal fit and low values of relative standard deviation for each parameter value.

RESULTS AND DISCUSSION

Experimental impedance spectra

Experimental IS of Pt/POEA electrode measured sequentially at 0.05 V are depicted in Fig. 3 as Bode (log $|Z_m|$ and ¨ *vs*. log μ) and Nyquist (Z_m" *vs*. Z_m') plots.

IS shown in Fig. 3 exhibit impedance/frequency responses typical for polyaniline based polymer films in transition oxidation states [34–37, 42–44]. Impedance increases in sequential measurements suggest significant time evolution of the system within operating time t_t of the impedance experiment [40–42]. The same is shown in Fig. 4, presenting t_t dependence of sequentially measured Nyquist plots in the form of 3-D plotting [16, 21].

Fig. 4 illustrates changes of sequentially measured IS with t_t referred to the beginning of the first IS measurement $t_{p(1)}$ = 0 (*cf*. Fig. 2). Each of the sequentially measured IS presented in Fig. 4 is seen as usual 2-D Nyquist plot (*cf*. Fig. 3b) presenting here for convenience data measured down to 0.25 Hz only, *i.e*. 56 frequency points between and 10^5 and 0.25 Hz. In agreement with the already shown Nyquist plots at EM→LE transition potentials of PANI [34–37], depressed semicircles at high to medium frequencies and capacitive lines at lower frequencies can clearly be recognized in Fig. 4. Obvious increase of circle diameters and capacitive lines with t_t suggests increased impedances in sequential measurements. This is also supported by bold lines drawn in Fig. 4 that connect impedances of each IS measured at the same *f* (1.58 Hz and 0.25 Hz) (iso-frequency points) and show continuously increased values with the operating time of the experiment. As in other cases of time changes of measured impedance [20,21], one might presume that time changes did not appear between measuremens only, but also during recording of each single IS that lasts for 19.7 minutes (*cf*. Fig. 1). This suggests that all experimental IS presented in Figs. 3 and 4 are nonstationary and should be corrected.

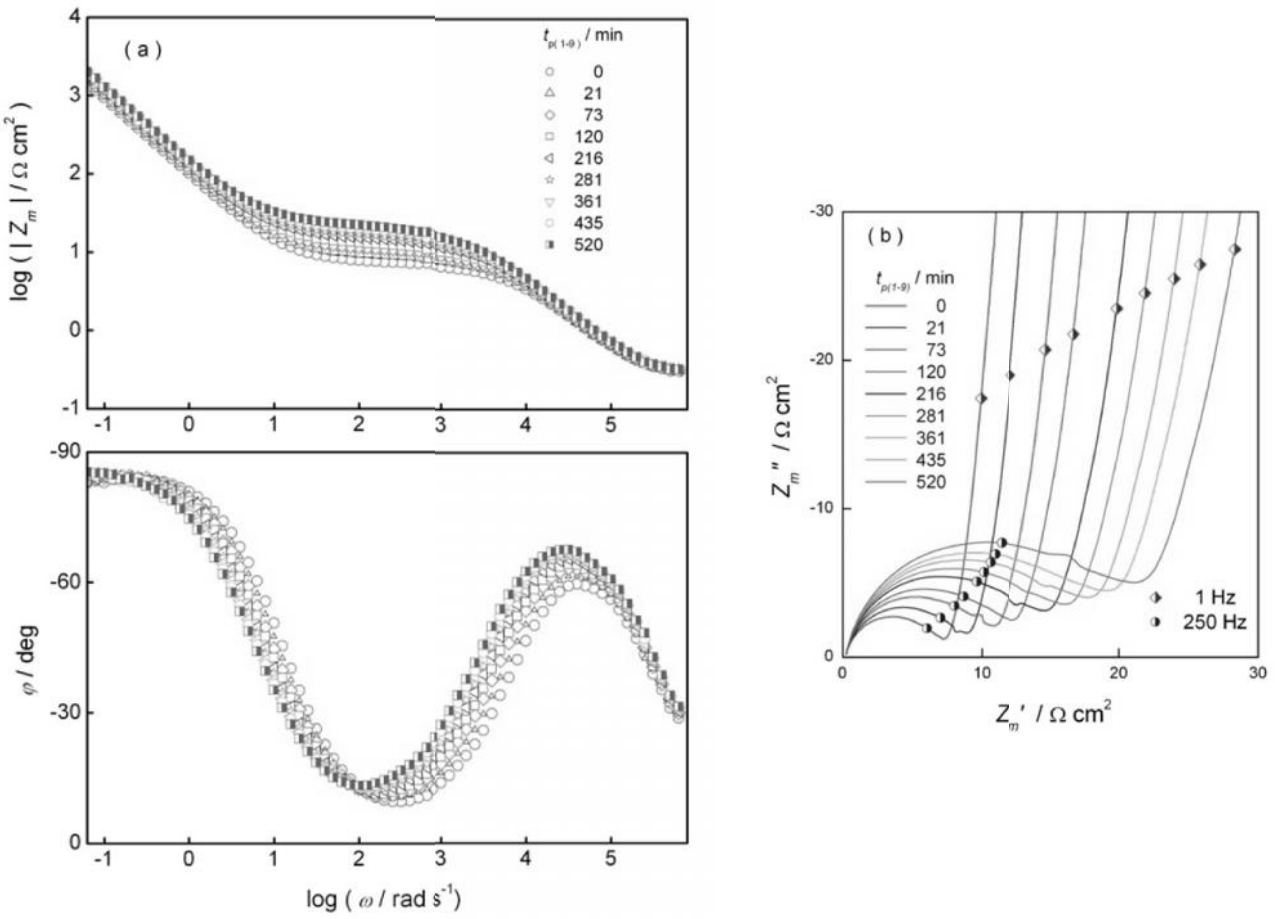

Fig. 3. (a) Bode and (b) Nyquist plots of sequentially measured IS of Pt/POEA electrode in 0.5 mol dm^{-3} H_2SO_4 at E = 0.05 V. $t_{p(1-9)}$ denote starts of 9 sequential IS measurements (*cf.* Fig. 2).

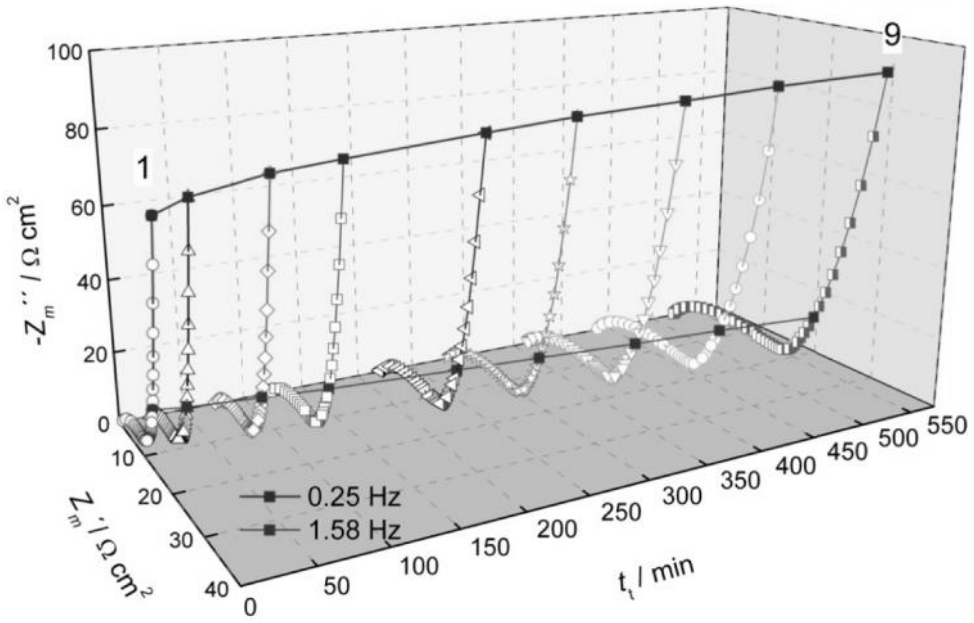

Fig. 4. 3-D presentation of Nyquist plots for sequentially measured IS (1–9) of Pt/POEA electrode in 0.5 mol dm^{-3} H_2SO_4 at E = 0.05 V. Iso-frequency points (1.58 Hz and 0.25 Hz) of 9 sequential IS are connected by bold lines

Implementation of Stoynov's 4-D analysis

Generation of instantaneous impedance spectra: According to Stoynov's 4-D analysis for correction of nonstationarity [12–14,24], each of the experimentally obtained data sets in a sequential series of conventionally measured IS has to be "frozen" in some well defined time. This procedure would give instantaneous IS, *i.e.* IS measured virtually for all frequencies at some strictly defined moment of time, *e.g.* starting time of IS measurement. The whole correction procedure is based on the assumption of continual impedance time change and is comprised from three steps of impedance data refinement.

In the first step of the correction procedure, each measured 4-D data set has to be transformed for the operating time t_t of sequential measurements, *i.e.* time elapsed from the start of the first IS measurement $t_{p(1)} = 0$. It is clear from Fig. 2 that each IS of the sequential series is actually measured at different time when referred to $t_{p(1).}$ This also implies different starting ($t_{s(1-71)}$), central ($t_{c(1-71)}$) and ending ($t_{e(1-71)}$) times of measurement at each frequency point (*cf.* Figs. 1 and 2). Selection of $t_{c(1-71)}$ values for further transformation is mostly justified, but needs additional calculations. According to Fig. 1 the central time of measurement at a given frequency $t_{c(n)}$ is defined as $t_{c(n)} = [t_{s(n)}+t_{e(n)}]/2$, or in the terms of $t_{e(n)}$ values that are available in experimentally obtained data sets, $t_{c(n)}=[t_{e(n-1)}+t_{e(n)+}t_d]/2$. Transformation for operating time t_t is made using calculated $t_{c(1-71)}$ and replacing $t_{e(1-71)}$ in experimentally obtained data sets by $t_{t(1-71)} = t_{p(1-9)} + t_{c(1-71).}$ In such a way the series of new 4-D data sets ($Z_m'_{(1-71)}$, $Z_m''_{(1-71),}$ $\mu_{(1-71)}$, $t_{t(1-71)}$) are formed for all 9 IS measured sequentially. Since t_t is referred to $t_{p(1)}=0$ at each frequency, the values of $t_{t(1-71)}$ are different for each of the sequentially measured IS.

In the second step of the correction procedure the mathematical function that properly describes the t_r changes of the measured impedance at all iso-frequency points has to be bulit up. The example presented in Fig. 5 shows $Z'_m(t_t)$ and $Z_m''(t_t)$ of sequentially measured IS at some frequencies chosen between 71 measured frequency points (iso-frequency dependences). .

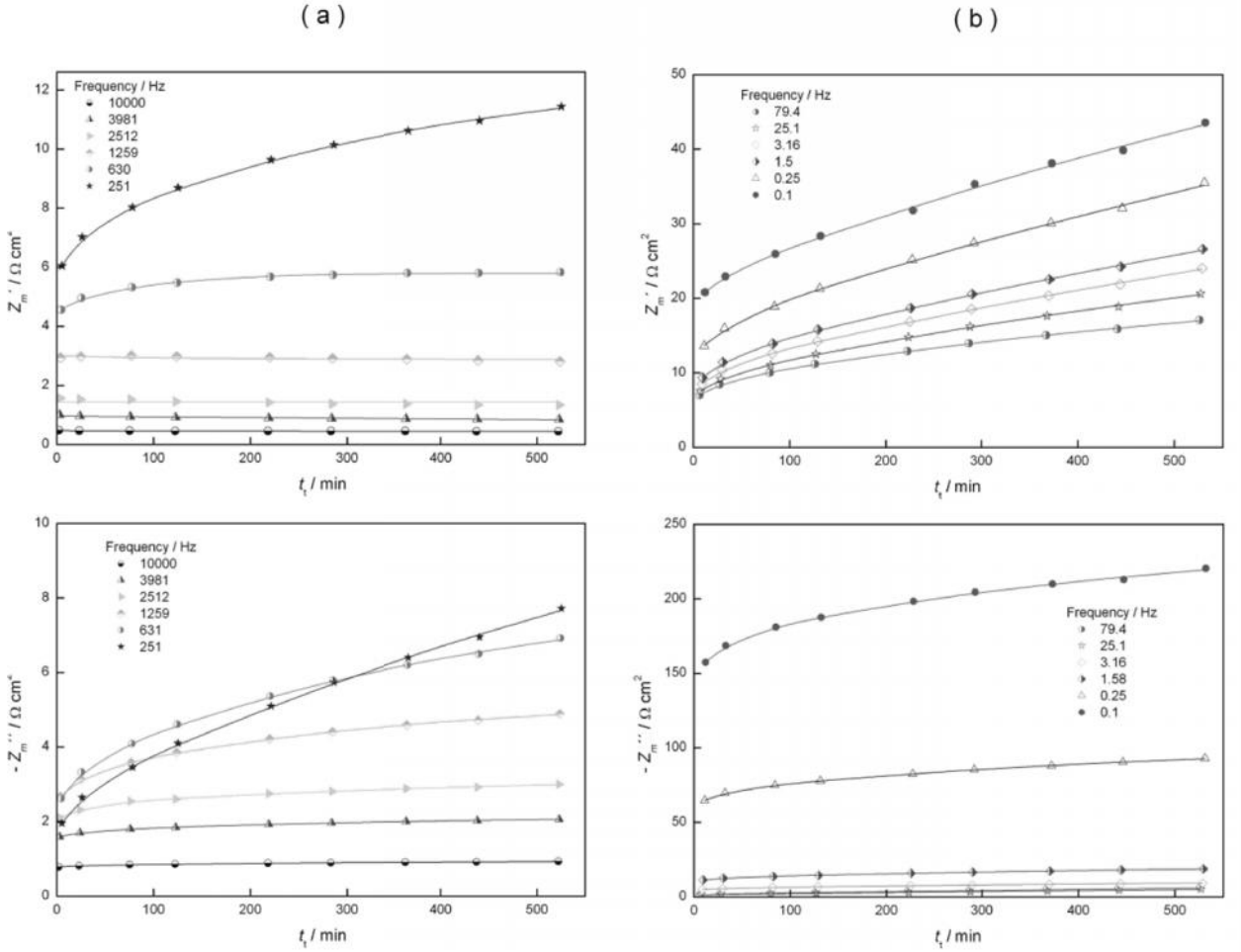

Fig. 5. Iso-frequency time dependences of Z_m' and Z_m'' of sequentially measured IS of Pt/POEA electrode in 0.5 mol dm^{-3} H_2SO_4 at E = 0.05 V. The chosen frequencies are divided to (a) high and (b) low range.

According to Fig. 5 the values of Z_m' and Z_m" increased with t_t and the changes are obviously higher between the first few IS than afterward. Taking into account different ordinate scales, Fig. 5 also shows more prominent changes at lower frequencies and higher changes in Z_m' than in Z_m" values. It has already been shown that just the time dependence of measured impedance at iso-frequency points makes the basis for calculations of IS at any desired time [12–14,21,22,24,41]. For further impedance data refinement, the proper impedance/time function has to be defined first. According to Stoynov [12–14,24] the piecewise polynomial function known as the complex spline, has proved to be appropriate. Here, temporal functions of Z_m' and Z_m" at each frequency in the time interval given in Fig. 5 were found well described (*cf.* full lines in Fig. 5) by the following combination of two exponential functions:

$$Z_m'(t_t) \text{ and } Z_m''(t_t) = A_0 + A_1(1-exp^{-t_t/T_1}) + A_2(1-exp^{-t_t/T_2}) \quad (2)$$

Eq. (2) is the multiparameter exponential function described by five constant parameters (A_0, A_1, A_2, T_1, T_2) that were for each of the 9 IS estimated separately for Z_m' and Z_m" at every second among the 71 frequency points. In such a way new data sets were obtained, containing numerical values of all five constant parameters (A_0, A_1, A_2, T_1, T_2) simulating $Z_m'(t_t)$ and $Z_m''(t_t)$ at 35 frequency points for each of the 9 IS.

In the third step of the correction procedure calculation of $Z_c(i\mu)$ in some "frozen" time t^* has to be performed using these new data sets. Here the values of Z_c' and Z_c" for each IS were estimated for $t^* = t_{p(1-9)} = 0$ by extrapolation/interpolation method and repeated for each frequency of the 35 frequency points. This step resulted ni the usual 3-D data sets ($Z_c'_{(1-35)}$, $Z_c''_{(1-35)}$, $\mu_{(1-35)}$) determining now 9 instantaneous IS, or in other words, 9 IS measured virtually at all frequencies just in the starting moments of the impedance measurements.

Comparison of measured and corrected impedance spectra: Nyquist plots of corrected impedances „frozen" at $t^* = t_{p(1-9)} = 0$ are presented in Fig. 6 together with the 1st, 2nd and 9th measured IS . In difference to Figs. 3 and 4, the measured IS in Fig. 6 are presented for every second of the 71 experimentally explored frequencies, *i.e.* for the same 35 frequency points for which calculations were performed.

The comparison between instantaneous, *i.e.* corrected for $t^* = t_{p(1-9)} = 0$ and measured IS in Fig. 6 shows differences that are higher for the first two than the last measured IS. Differences are primarily seen as different impedance values and are particularly obvious at medium and low frequency regions.

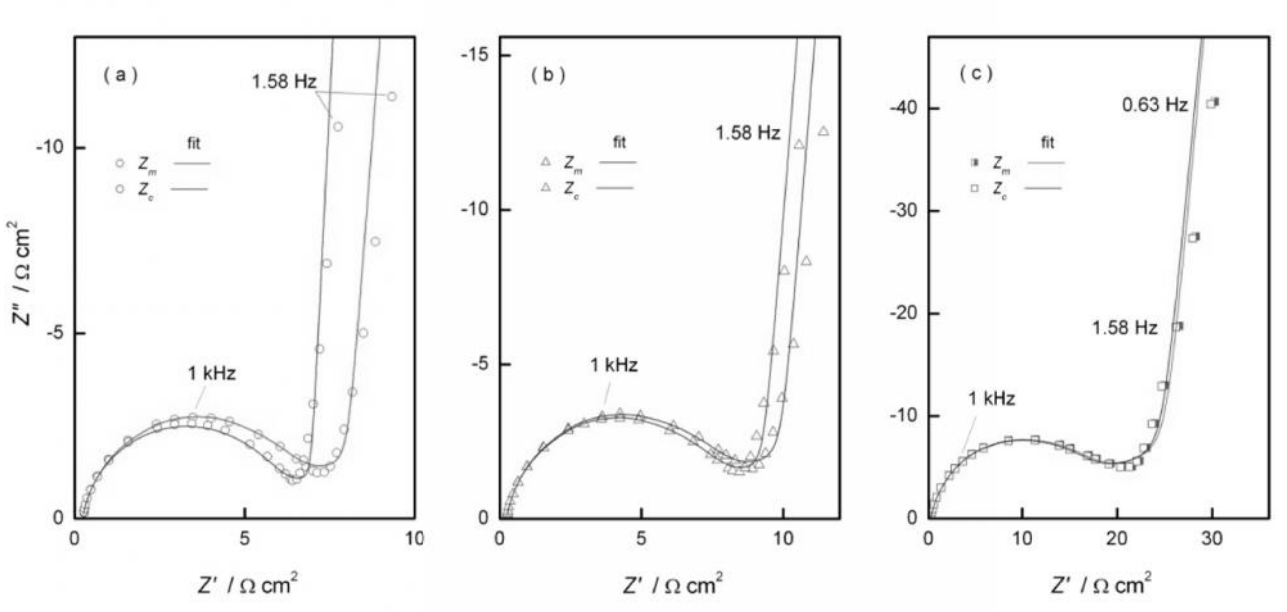

Fig. 6. Measured and corrected ($t^* = t_{p(1-9)}=0$) Nyquist plots of (a) 1st, (b) 2nd and (c) 9th IS of Pt/POEA electrode in 0.5 mol dm^{-3} H_2SO_4 at E = 0.05 V.

Instantaneous IS showed generally lower semicircle diameters and lower capacitive lines (*cf.* Z" values at the same f = 1.58 Hz), indicating different quantitative impedance parameter values describing characteristic Pt/POEA electrode properties. In terms of the usual model for metal/PANI/solution electrode arrangement comprising interfacial double-layer capacitance,

interfacial charge transfer resistance and charge transport within polymer film [38,40,42–44], overvestimation of all charge transfer and charge transport resistances and underestimation of charge pseudocapacitance values for not corrected IS of Pt/POEA electrode have strongly been indicated.

Not only measured, but also instantaneous IS change with time suggests that Pt/POEA electrode is inherently time-varying system. These time variations can be related to electrochemical aging, the phenomenon generated by polymer volume decrease at EM→LE conversion, what has already been found characteristic for PANI and PANI based derivatives [41,47].

CONCLUSIONS

Stoynov's 4-D model was successfully applied for corrections of nonstationary impedance spectra of the Pt/POEA electrode measured in acid sulphate solution at the potential of transition between the conducting and insulating state of the polymer. The conventional FRA based EIS technique was used and the experiment was performed as series of 9 sequentially measured impedance spectra in the total operating time of 540 min. Measured impedance spectra of Pt/POEA electrode showed continuous increase with operating time, including changes within time interval of one single impedance spectrum measurement of 19.7 min, indicating nonstationarity.

To account for nonstationarity, experimental data sets of the series of sequentially measured impedance spectra must be obtained in 4-D form. In comparison with ordinary 3-D data set ($Z'_{(n)}$, $Z''_{(n)}$, $\mu_{(n)}$), 4-D form must involve some specific time variable. Here, a specific time moment, defined as the central time of data acquisition at each measured frequency point $t_{c(n)}$ is calculated and involved as the fourth variable in experimental 4-D data sets ($Z'_{(n)}$, $Z''_{(n)}$, $\mu_{(n)}$, $t_{c(n)}$) of each measured impedance spectrum.

Correction procedure has to be applied in several steps. As a first step $t_{c(n)}$ values of each impedance spectrum must be referred to the operating time of the experiment. After that, iso-frequency dependences of measured real and imaginary impedance parts of all measured impedance spectra must be extracted and their changes with operating time simulated by implementing of proper mathematical function. Here combination of two exponentials providing five constant parameters for each frequency point was found satisfactory. Thus, the obtained constant parameter values and the extrapolation/interpolation method were in turn used for calculations of 3-D data sets ($\mu_{(n)}$, $Z'_{(n)}$, $Z''_{(n)}$) of instantaneous IS, *i.e.* IS "frozen" to the starting time of each impedance spectrum measurement.

Comparison between experimentally measured and instantaneous impedance spectra pointed to overvestimation of all charge transfer and charge transport resistance values and underestimation of charge pseudocapacitance values for IS of Pt/POEA electrode not corrected for nonstationarity.

Acknowledgements: *This work is supported by the Croatian Science Foundation under the project ESUP-CAP (IP-11-2013-8825).*

REFERENCES

1. M. Sluyters-Rehbach, J.H. Sluyters, Sine wave methods in the study of electrode processes, in: A.J. Bard (ed), Analytical Chemistry, M. Dekker, New York, 1970, p. 1.
2. A. Lasia, Electrochemical impedance spectroscopy and its application, in: R.E. White, B.E. Conway and J. O Bockris (eds), Modern aspects of electrochemistry, Kluwer Acad. Publ., New York, 1999.
3. E. Barsoukov and J. R. Macdonald (eds), Impedance spectroscopy: Theory, experiment and applications, J. Willey & Sons, 2005.
4. M.E. Orazem, B. Tribollet, Electrochemical impedance spectroscopy, J. Willey & Sons, 2008.
5. B.-Y. Chang, S.-M. Park, *Annu. Rev. Anal. Chem*., **3,** 207 (2010).
6. P. Zoltowski, *Bulg. Chem. Commun*., **44**, 383 (2012).
7. K. Darowicki, *Electrochim. Acta*, **40**, 439 (1995).
8. G.S. Popkirov, *Electrochim. Acta*, **41**, 1023 (1996).
9. E. Barsoukov, S.-H. Ryu, H. Lee, *J. Electroanal. Chem*., **536**, 109 (2002).
10. E. Van Gheem, R. Pintelon, J. Vereecken, J. Schoukens, A. Hubin, P. Verboven, O. Blajiev, *Electrochim. Acta*, **49**, 4753 (2004).
11. J. R. Wilson, D.T Schwartz, S.B. Adler, *Electrochim. Acta*, **51**, 1389 (2006).
12. Z. B. Stoynov, B. Savova-Stoynov, *J. Electroanal. Chem*., **183**, 133 (1985).
13. B. Savova-Stoynov, Z. B. Stoynov, *Electrochim. Acta*, **37**, 2353 (1992).
14. Z. Stoynov, *Electrochim. Acta*, **38**, 1919 (1993).
15. K. Darowicki, P. Ślepski, *Electrochim. Acta*, **49**, 763 (2004).
16. P. Ślepski, K. Darowicki, E. Janicka, G. Lentka, *J. Solid State Electrochem*., **16**, 3539 (2012).
17. T. Breugelmans, J. Lataire, T. Muselle, E. Tourwé, R. Pintelton, A. Hubin, *Electrochim. Acta*, **76**, 375 (2012).
18. F. Berthier, J.-P. Diard, A. Jusssiaume, J.-J. Rameau, *Corr. Sci*., **30**, 239 (1990).
19. M. A. Vorotyntsev, M. D. Levi, A. Schechter, D. Aurbach, *J. Phys. Chem. B*, 1**05,** 188 (2001).
20. C.A. Schiller, F. Richter, E. Gülzow, N. Wagner, *Phys. Chem. Chem. Phys*., **3**, 374 (2001).

21. N. Wagner, E. Gülzow, *J. Power Sourc*., **127**, 341 (2004).
22. Z. Stoynov, D. Vladikova, Differential impedance analysis, Marin Drinov Acad. Publ. House, Sofia, 2005.
23. G. Raikova, Z. Stoynov, D. Vladikova, in: Advanced Techniques for Energy Sources Investigation and Testing, Proc. Int. Workshop, P18-1 (2004).
24. Z. Stoynov, B. Savova-Stoynov, T. Kossev, *J. Power Sourc*., **30**, 275 (1990).
25. J. Pouget, S.LZhao, Z.HWang, Z. Oblakowski, A. Epstein, S. Manobar, J. Wiesinger, A. Macdiarmid, C. Hsu, *Synth. Met*., **55**, 341 (1993).
26. A. MacDiarmid, *Angew. Chem. Int. Ed*., **40**, 2581 (2001).
27. G. Inzelt, M. Pineri, J.W. Schultze, M.A.Vorotyntsev, *Electrochim. Acta* **45**, 2403 (2000).
28. M. Grzeszczuk, P. Poks, *Synth. Met*., **98**, 25 (1998).
29. E. Csahók, E. Vieil, G. Inzelt, *J. Electroanal. Chem*., **482**, 168 (2000).
30. R. Mažeikienė, A. Malinauskas, *Synth. Met*., **123**, 349 (2001).
31. X. Yang, Q. Xie, S. Yao, *Synth. Met*., **143**, 119 (2004).
32. J. Yoo, I. Song, J. Lee, S. Park, *Anal. Chem*., **75**, 2962 (2003).
33. K. Darowicki, J. Kawula, *Russ. J. Electrochem*., **41**, 1055 (2007).
34. I. Rubinstein, E. Sabatani, J. Rishpon, *J. Electrochem. Soc*., **134**, 3078 (1987).
35. H. Dinh, P. Vanysek, V. Birss, *J. Electrochem. Soc*., **146**, 3324 (1999).
36. C.-C. Hu, C.-H. Chu, *J. Electroanal. Chem*., **503**, 105 (2001).
37. S. Mondal, K. Prasad, N. Munichandraiah, *Synth. Met*., **148**, 275 (2005).
38. V. Horvat-Radošević, K. Kvastek, M. Kraljić Roković, *Electrochim. Acta*, **51**, 3417 (2006).
39. M.C.E. Bandeira, R. Holze, *Microchim. Acta*, **156**, 125 (2007).
40. M. Žic, *J. Electroanal. Chem*., **610**, 57 (2007).
41. W.A. Marmisollé, M. I. Florit, D. Posadas, *J. Electroanal. Chem*., **673**, 65 (2012).
42. V. Horvat-Radošević, K. Kvastek, *J. Electroanal. Chem*., **631**, 10 (2009).
43. V. Lvovich, Electrochem. Soc. Interface, 62 (2009).
44. J. Rubinson, Y. Kayinamura, *Chem. Soc. Rev*. **38**, 3339 (2009).
45. V. Horvat-Radošević, K. Kvastek, *J. Electroanal. Chem*., **591**, 217 (2006).
46. M. Kraljić Roković, L. Duić, *Electrochim. Acta*, **51**, 6045 (2006).
47. W. Marmisollé, D. Posadas, M. Florit, *J. Phys. Chem. B*, **112**, 10800 (2008).

ПРИЛАГАНЕ НА 4-D ИМПЕДАНСЕН АНАЛИЗ НА СТОЙНОВ ЗА КОРЕКЦИИ НА НЕСТАЦИОНАРНИ ИМПЕДАНСНИ СПЕКТРИ НА ТЪНЪК ПОЛИ(О-ЕТОКСИАНИЛИН) МОДИФИЦИРАН Pt ЕЛЕКТРОД

В. Хорват-Радошевич*, К. Квастек, К. Магдич Кошичек

Лаборатория по морски изследвания и опазване на околната среда, Институт „Р. Бошкович“, Биеничка 54, 10000 Загреб, Хърватия

Постъпила на 18 ноември 2016 г.; коригирана на 2 януари 2017 г.

(Резюме)

Приложен е 4-D анализа на Стойнов за корекции на нестационарни импедансни спектри на поли (о-етоксианилин) POEA модифициран Pt електрод измерен чрез конвенционалната техника на ЕИС при потенциала на конверсия на полимера от проводник в изолатор. Серия от девет последователно измерени импедансни спектри (ИС) на Pt / POEA електрод показват значително развитие с нарастване продължителността на експеримента, което предполага измерването на система, която не само варира с времето, но е и нестационарна, т.е. променяща се по време на снемане на единичния импедансен спектър. Беше приложена процедура за корекция на нестационарността, състояша се от три математически стъпки, приложени към всеки от последователно измерените импедансни спектри. В първата стъпка на процедурата като четвърта променлива включена в набора от импедансни данни за всички експериментално измерени импедансни спектри бяха определени централните времена за събиране на данни от всяка честотна точка, отнасящи се към времето на провеждане на експеримента. Във втората стъпка на процедурата времевата оперативна функция на измерените реална и имагинерни импедансна компоненти при изо-честотни точки бе построена и „замразена“ спрямо началното време на измерване на всеки импедансен спектър.В последната стъпка от процедурата бяха изчислени девет моментни импедансни спектри чрез използване на метода на екстраполация/интерполация. Сравняването на измерените с моментните импедансни спектри показа разлики, които предполагат повишена оценка на съпротивлението на преноса и транспорта на заряд и понижени стойности на псевдо-капацитета за не-коригирани спрямо коригиран ИС на Pt / POEA електрод.